JOURNAL OF APPLIED ELECTROCHEMISTRY 8 (1978) 333–345

Electro-oxidation of ammonia in waste water

L. MARINČIĆ*, F. B. LEITZ†
Ionics Inc., Watertown, Mass., USA

Received 25 October 1977

A study was undertaken of the electro-oxidation of ammonia as a possible new method of ammonia removal during waste-water treatment. Reaction rates were measured in the concentration range of $1{\cdot}2 \times 10^{-4}$ M to 1×10^{-2} M ammonia and at pH values of 5–13. The influence of the polarization rate ($0{\cdot}05$–$0{\cdot}5$ V min^{-1}) and the ammonia concentrations on the oxidation peak current were studied. A number of electrocatalysts were evaluated and most favourable potentials were determined using a conventional three electrode electrolytic cell.

Performance data are presented from a continuous flow bench scale electrolytic cell with a 90 cm path length working at various experimental conditions.

1. Introduction

Previous investigators [1–5] have demonstrated that ammonia is oxidized to nitrogen on platinum black anodes from strongly alkaline solutions containing high concentrations of ammonia. The kinetics of the reaction are in dispute, but there is general agreement that the overall electrochemical reaction proceeds with a three-electron exchange yielding nitrogen and water with almost 100% faradaic efficiency:

$$NH_3 + 3\,OH^- \rightarrow 1/2N_2 + 3H_2O + 3\,e^-. \quad (1)$$

On other catalysts, nitrates and nitrites were also observed as reaction products [3, 6, 7].

The objective of the present investigation is to examine the anodic oxidation of ammonia as a possible new method of ammonia removal from waste water during secondary sewage treatment. An acceptable new method should have economic advantages over present methods: air stripping at high pH, bio-oxidation to nitrates and breakpoint chlorination, none of which are considered entirely satisfactory at this time.

It should be emphasized that this work was designed to determine the feasibility of the ammonia oxidation process under conditions expected at sewage effluents (ammonia concentration 5×10^{-4} M–2×10^{-3} M and pH 5–8 with nitrogen and water as the only products. Any other oxidation products would be considered to be as seriously polluting as ammonia.

No attempt was made to conduct kinetic studies involving the various intermediates in the oxidation process or to determine what the reaction steps or intermediate products were.

A search for an economic, active catalyst was carried out after the feasibility of the process and general conclusions were established using a platinized platinum black catalyst.

2. Experimental

Experiments were conducted at room temperature in various supporting electrolytes (NaCl, K_2SO_4, KOH, phosphate buffer and K_2HPO_4) with pH values varying from 5·55–12·8 and ammonia concentration from $1{\cdot}2 \times 10^{-4}$ M to 1×10^{-2} M ($\sim$ 2–170 mg l^{-1}).

The experimental work included three different parts: qualitative or micro-experimental part, quantitative or macro-experimental part and finally, the cell performance experiments obtained with a continuous flow bench scale electrolytic cell.

2.1. *Micro-experimental set-up*

An all glass, two compartment, three electrode electrochemical cell of conventional design was

---

[*] Present address: E. P. Joslin Research Laboratory, Harvard Medical School, Boston, Mass. USA
[†] Present address: Bureau of Reclamation, Denver, Colorado, USA

Printed in Great Britain.

used. The central compartment of the cell contained the working electrode and had a sufficient volume to minimize concentration changes during the experiments. The working electrode was platinized platinum (bulb-type rotating electrode after Laitinen–Kolthoff) assembled with a Sargent constant-speed stirring motor ($N = 10$ rev s^{-1}). A standard electrode cleaning treatment [8] was used prior to platinization, and the same standard platinizing procedure [8] yielding velvety-black deposits was used before each set of measurements. The geometric area of the electrode was 0·13 cm^2. All currents are quoted on the basis of geometric area.

In electrocatalyst screening experiments, the platinized platinum micro-electrode was replaced with some other metals, bright or black noble metals and powder-type catalysts of different composition layered over the inert base metal. These experiments were conducted at room temperature in a phosphate buffer solution of pH = 8·00 ± 0·15 with helium gas bubbling through the cell. The ammonia concentration was 50–100 mg l^{-1}.

Test electrodes were prepared from high purity material 0·010–0·020 in wires (from A. D. McKay, Inc.) which were sealed into glass tubing. Electrical contact was established through a column of mercury inside the glass tubing and all prepared electrodes were tested at a rotating velocity (N) of 10 rev s^{-1}.

The procedure used for preparation of platinized graphite was the same one as for platinum.

The electrodes for testing electrocatalysts in powdered form were prepared by coating titanium wire (0·02 in) or titanium plate as a substrate metal with a mixture of powdered catalyst and binder (Teflon T-30 dispersion). The pretreatment of titanium consisted of cleaning in hot (70° C–boiling) hydrochloric acid (8–12 N) for 5–15 min. Graphite and tungsten bronzes were often used in the mixture with the catalyst to improve the electrical conductivity and to dilute the expensive catalyst.

It has been shown that by incorporation of tungsten bronze into the platinum black anodes, the electro-oxidation of carbon monoxide and reformer gas can be appreciably enhanced [9]. An attempt was made to use platinum catalyst more effectively in the ammonia oxidation reaction by addition of tungsten bronzes to the catalyst in different ratios.

Sodium tungsten bronzes with the general formula Na_xWO_3 and high sodium content were prepared according to a modified Straumanis [10] procedure.

Platinum electrodeposition on titanium and tantalum was carried out using the same procedure as for platinizing platinum. Tantalum electrodes were treated prior to platinization by applying a current of 100 mA cm^{-2} for 15 min in 2% sulphuric acid solution. Titanium was pretreated in hot hydrochloric acid in the same way as for powder-catalyst electrode preparation.

The platinized platinum gauze counter-electrode was separated from the main compartment by a fritted glass. The reference electrode was Hg/HgO electrode in 1 M KOH and in some experiments saturated calomel electrode.

All potentials are referred to the standard hydrogen electrode (SHE).

Potentiodynamic procedures have been employed in most of this work using a Heath Polarography System Model EUW-YO1.

The potential–time sequence applied to the test electrode prior to recording the current–potential data proceeded as follows:

(a) A cleaning potential pulse was applied starting from the hydrogen evolution potential; it was held at the oxygen evolution potential for 1 min and reversed.

(b) The electrode was held at the initial potential (hydrogen evolution potential) for 3 min.

(c) Applying the potential sweep (– 0·2 V → + 1·0 V → – 0·2 V) at a selected sweep rate without recording currents.

(d) Three minute equilibration at initial potential (– 0·2 V).

(e) Recording the current–potential data at a selected sweep rate.

In some experiments the 'steady-state' measurements were also made. The current–potential relationship was determined point by point at 20 mV steps and controlled intervals of time (1 min). Potentiostatic measurements were performed at several predetermined polarization potentials to establish the effect of time on the oxidation rate.

2.2. *Macro-experimental set-up*

To determine the course of the reaction, experiments were continued with a larger platinized platinum electrode and reaction products accumulated for analysis. The apparatus consisted of an air-tight Pyrex glass cell with a rotating platinized platinum gauze anode (geometrical surface area 20 cm^2), mercury (triply distilled) cathode, Hg/HgO reference electrode, sweep-gas inlet, solution overflow outlet, and gas and solution sampling outlet. The solution content was 1·2 l. The supporting electrolyte was a phosphate buffer (pH 8·2) and the initial ammonia concentration varied from 40–55 mg l^{-1}.

The initial experimental step was pre-electrolysis in the supporting electrolyte at 1–2 mA for 2 hours. Helium gas was bubbled through the cell for at least two hours, before the experiment was started, to exclude the air from the solution and to replace the air at the top of the cell. Flushing was continued until very little air was detected in the cell by chromatographic analysis. After flushing, the ammonia was added and the experiment started by applying the current of 15–20 mA. The corresponding anodic potential was kept in this way all the time below the critical point, where anode passivation occurs. Samples of solution and gas were taken for analysis every 1–2 hours. Tests on the most probable reaction products (nitrates, nitrites, hydrazine and hydroxylamine in solution, and nitrogen in gas phase) and determination of ammonia concentration changes during the oxidation reaction were made. The minimum detectable ammonia nitrogen concentration was 0·1 mg l^{-1}, nitrite nitrogen 0·01 mg l^{-1}, nitrate nitrogen 0·2 mg l^{-1} and hydrazine 0·01 mg l^{-1}.

Chromatographic analysis of the gaseous phase was conducted using an Aerograph Gas Chromatograph Model A-90-P3.

2.3. *Continuous flow bench scale electrolytic cell*

A continuous flow electrolytic cell was used to simulate one of many parallel channels in a full size prototype. The cell contained a platinized titanium anode and stainless steel cathode with the cell volume and active electrode surface area being defined by a polyethylene spacer between the electrodes. A top view and a cross-section of the spacer is shown in Fig. 1. The active electrode area in the cell was 63 cm^2 with a flow path length of 90 cm and a path width of 0·7 cm. No membrane or diaphragm was used to separate the electrodes. A test solution was prepared from ammonia and a pH buffer at values typical of waste-water effluents (about 30 mg l^{-1} ammonia, pH 8).

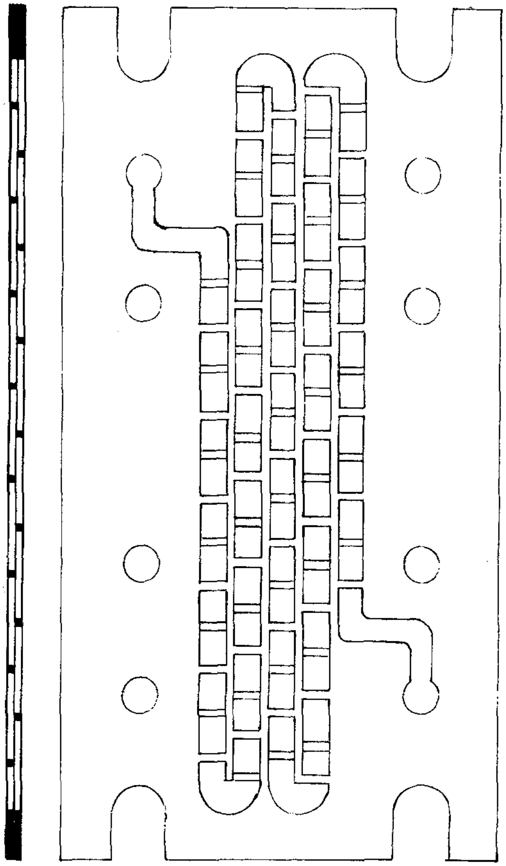

Fig. 1. Top view and the cross-section of the tortuous path spacer.

The experimental set-up consisted of a feed solution reservoir containing 13 l of test solution. The solution was fed to the cell by a centrifugal pump. A rotameter, calibrated by effluent collection, measured the flow rate. Current was provided by a 25 A d.c. power supply.

The experimental parameters were selected on the basis of a design equation (Equation 4). With the assumption of 50% average current efficiency and 90% ammonia concentration reduction (from 2×10^{-3} M or 34 mg l^{-1} to 2×10^{-4} M or 3·4 mg l^{-1}) and the tortuous path spacer of 90 cm length and 0·1 cm thickness, a linear velocity of 0·274 cm s^{-1} was required with a corresponding retention time of 327 s.

The experimental data were recorded with

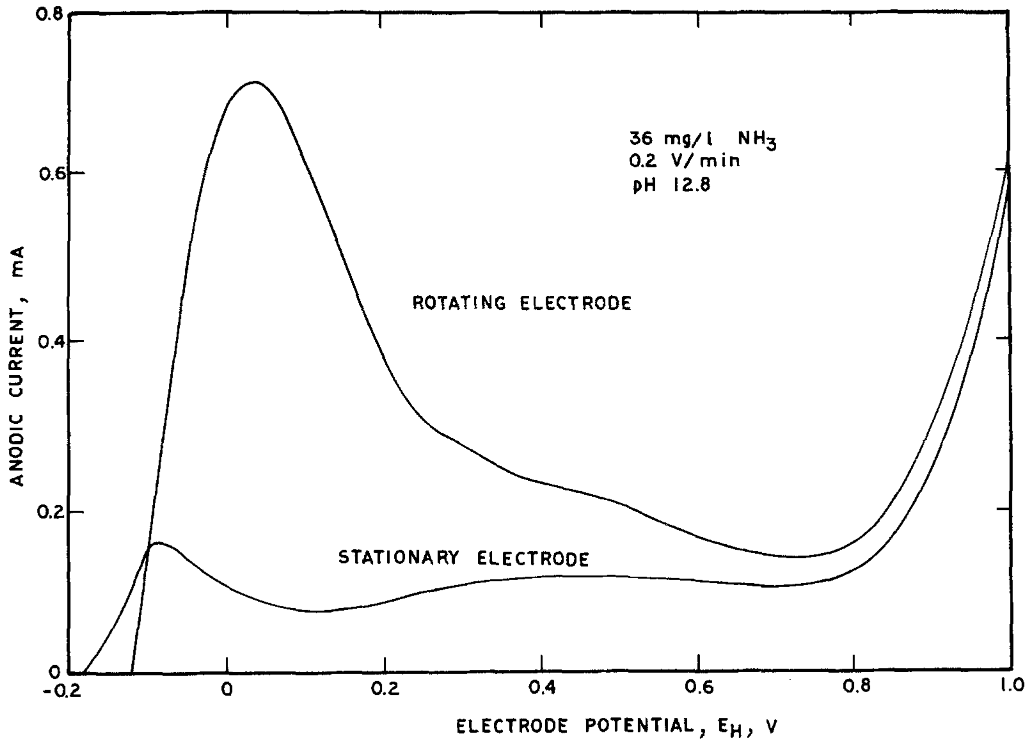

Fig. 2. Current–potential curves obtained with rotating and stationary electrodes.

Table 1. Peak currents for the stationary and rotating platinized platinum electrode at pH 12·8

Sweep rate (V min^{-1})	*Ammonia concentration* ($C \times 10^3$, mol l^{-1})	*Peak current density* (mA cm^{-2}) *Rotating*	*Stationary*
0·50	3·2	11·2	2·20
	1·6	6·4	1·31
	1·0	3·8	1·13
0·2	3·2	8·4	1·23
	1·4	4·8	0·72
	1·1	2·7	0·70
0·1	3·1	7·5	0·99
	1·5	4·2	0·58
	0·9	2·3	0·46
0·05	2·8	5·9	0·82
	1·5	3·2	0·46
	1·0	2·2	0·39
‘steady-state’	3·0	4·6	0·67
	1·4	2·5	0·37
	0·8	1·7	0·20

various solution feed rates, spacer thicknesses and current densities.

3. Results and discussion

3.1. *Platinized platinum micro-electrode*

Current–potential curves recorded during a single linear anodic potential sweep with stationary and rotating platinized platinum electrode are shown in Fig. 2. In both cases an anodic current peak appears prior to the formation of platinum surface oxides. The current peak obtained with a rotating electrode is slightly shifted towards more positive potentials (0·05 V versus – 0·1 V for stationary electrode) and the intensity of current at the maximum is considerably increased when mass transfer was enhanced by the electrode rotation.

Table 1 shows the peak currents for stationary and rotating platinized platinum electrodes which were measured at various sweep rates and various ammonia concentrations. Some typical current–potential curves recorded with a rotating electrode are shown in Fig. 3. The lowest of the set of curves in each graphical presentation in this figure was recorded in a supporting electrolyte (0·1 M KOH, pH 12·8) without the addition of ammonia. The sweep started at the potentials where the electrode surface is free from both adsorbed hydrogen and oxygen. The ammonia oxidation rates are increasing with increased ammonia concentration and increased potential sweep rate.

The current–potential curves recorded point by point at 'steady-state' conditions are shown in Fig. 4. Current peaks observed at about 0·025 V versus SHE are increasing with concentration in the same manner as in the potentiodynamic experiments.

Anodic current density as a function of ammonia concentration is plotted in the graph shown in Fig. 5. A linear relationship exists between the anodic current density (measured at the current peak) and ammonia concentration over the concentration range 7·5 x 10^{-4}–3·0 x 10^{-3} M.

Peak current densities are plotted versus the square root of the potential sweep rate in Fig. 6. A linear relationship is observed at four different ammonia concentrations.

The effect of pH on the peak current density

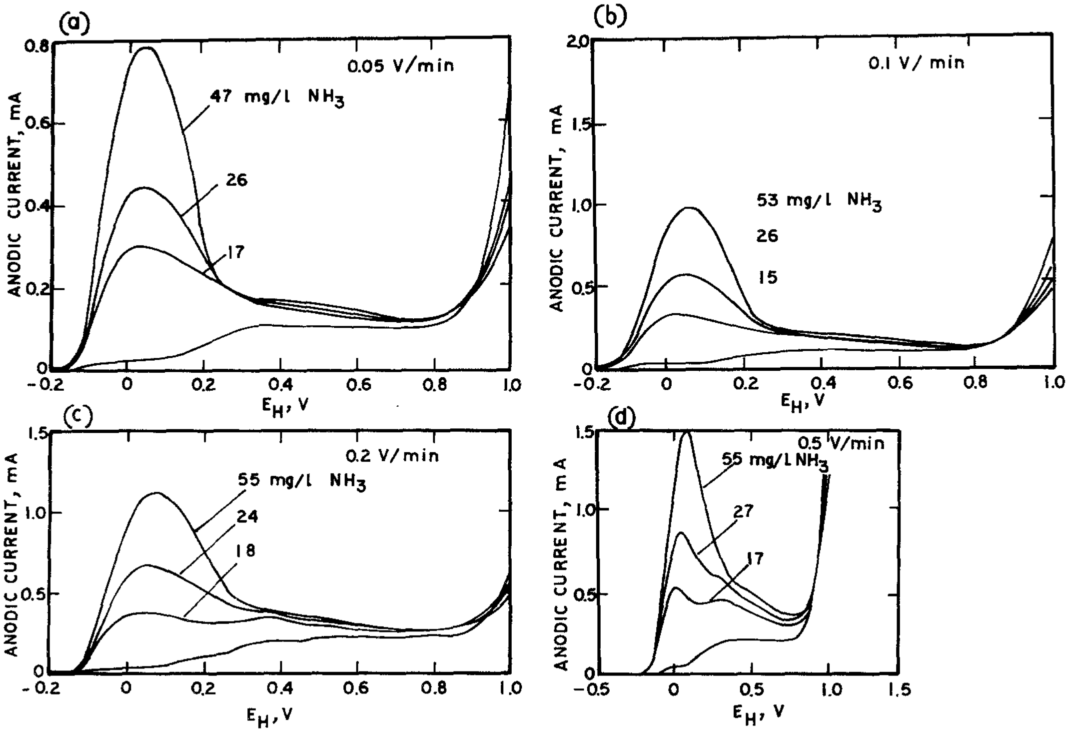

Fig. 3. Current–potential relationship for various ammonia concentrations. pH 12·8, rotating Pt–Pt electrode. (a) Sweep rate 0·05 V min^{-1}, (b) Sweep rate 0·10 V min^{-1}, (c) Sweep rate 0·20 V min^{-1}, (d) Sweep rate 0·50 V min^{-1}.

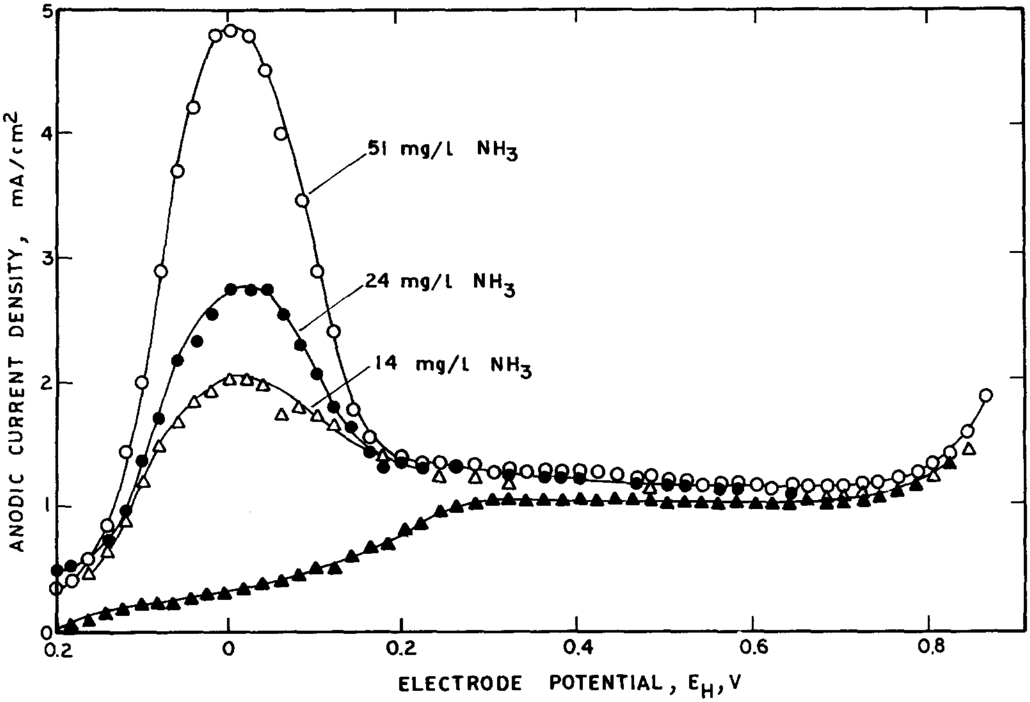

Fig. 4. Current–potential relationship for various ammonia concentrations from steady-state measurements. pH 12·8, rotating Pt–Pt electrode.

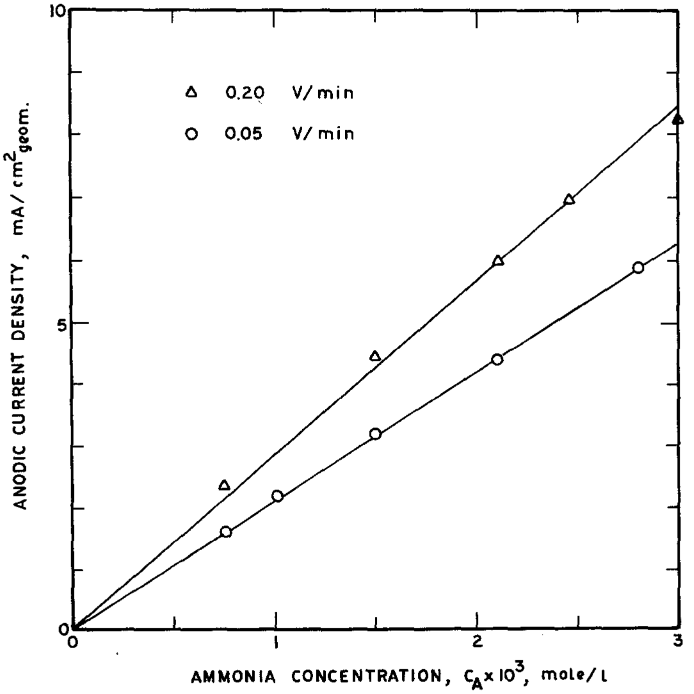

Fig. 5. Current density as a function of the ammonia concentration. pH 12·8, rotating Pt–Pt electrode.

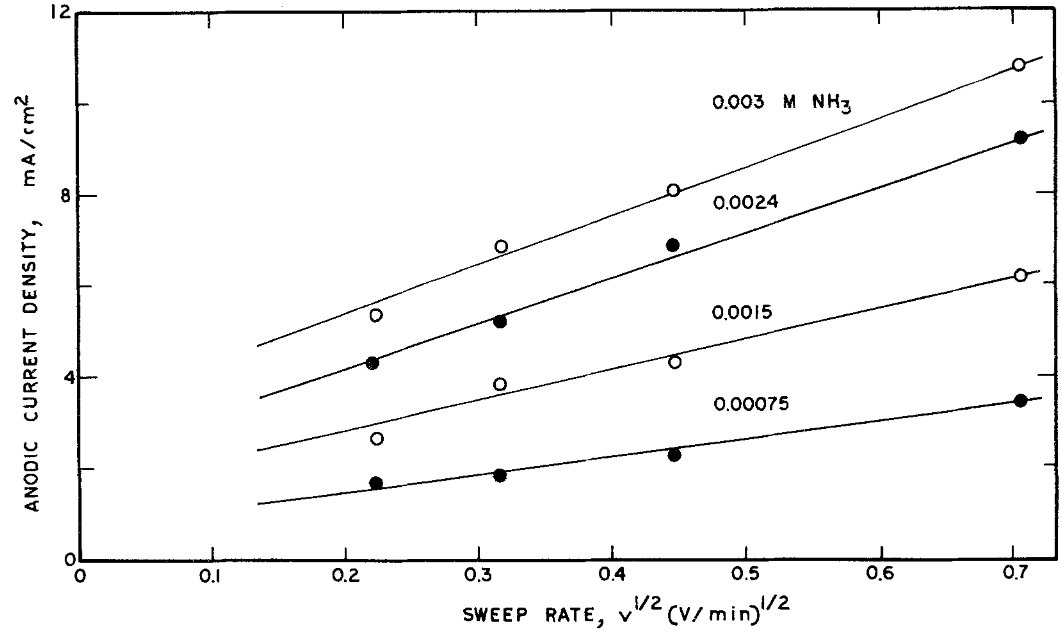

Fig. 6. Effect of the sweep rate on the anodic current density. pH 12·8, rotating Pt–Pt electrode.

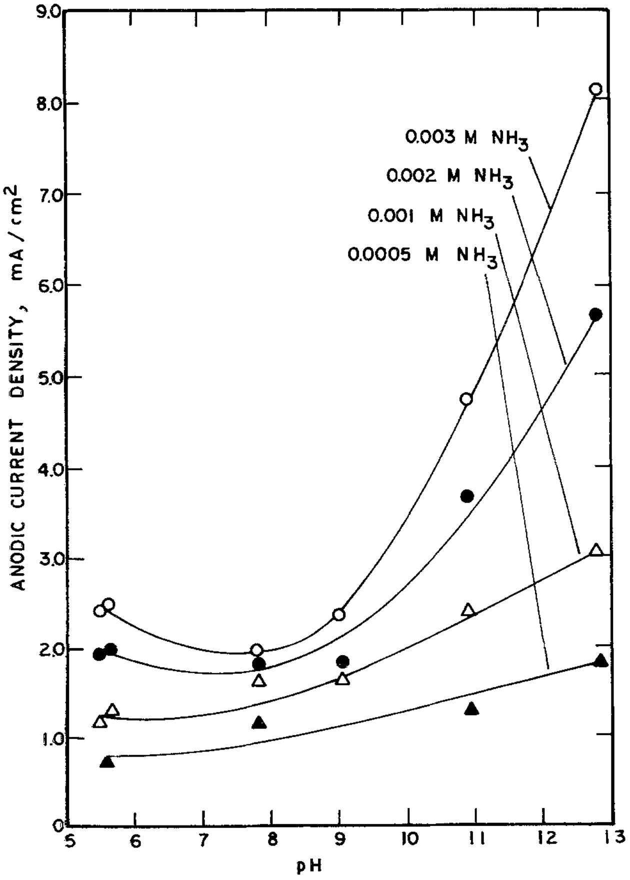

Fig. 7. Effect of pH on the peak current density at sweep rate of 0·2 V min^{-1}, rotating Pt–Pt electrode.

was determined by conducting the experiments under the same experimental conditions but with a supporting electrolyte of different pH value. The pH range 5·5–12·8 was investigated with the corresponding peak current densities presented in the graph shown in Fig. 7. The pH dependence is very moderate at low ammonia concentrations and the current density–pH correlation is close to linear. At higher concentrations the current density–pH curve shows a minimum between pH 8 and 9 and then current densities increase considerably with increasing pH values and moderately with decreasing pH values. Shifts of the current peak potentials towards more positive potentials were observed with decreasing pH values.

The potentiostatic current–time curves were recorded at pH 9·05 with varying ammonia concentration and at several predetermined protentials. The potentials chosen were: one at the ascending, one at the descending, and one at the peak position of the current–potential curves. The current–time relationships at these potentials, recorded for a duration of 5 min, are shown in Fig. 8. The ammonia oxidation rate, as a function of time, remains constant in the narrow range of potentials (100–300 mV versus SHE), where apparently no decrease of the active sites at the electrode surface occurs after prolonged polarization time. At the potential of the current peak and more positive potentials a considerable current decay with time is observed.

3.1.1. Electrocatalyst evaluation. The main emphasis was on investigation of noble metal catalysts and this work revealed platinum as the only material which would sustain a satisfactory current density. Table 2 gives the comparison of

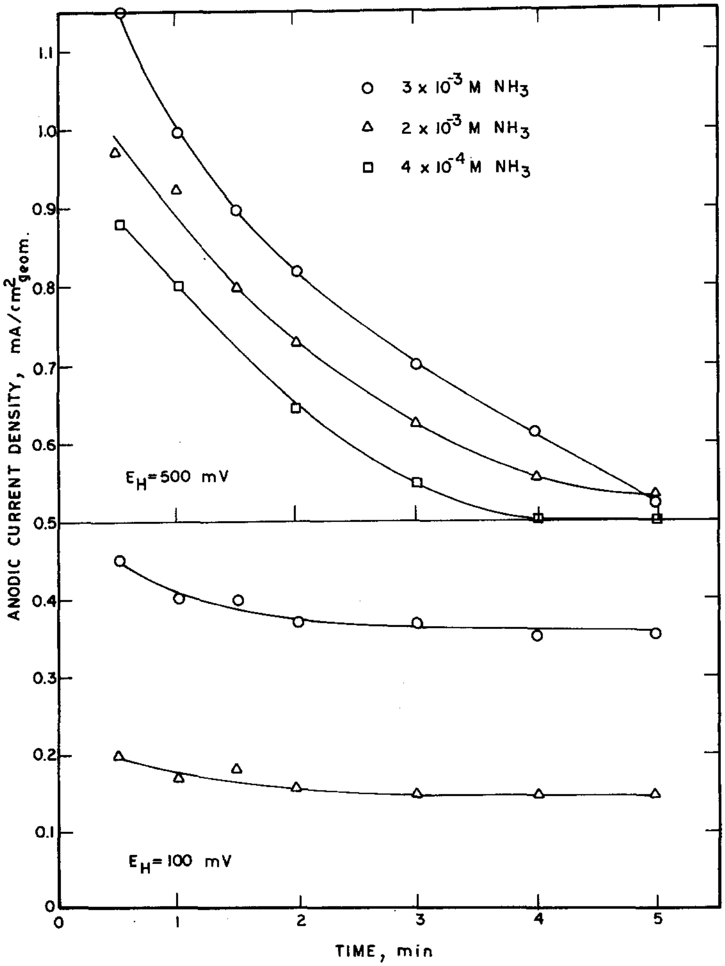

Fig. 8. Potentiostatic current–time curves at 500 mV and 100 mV versus SHE. pH 9·05, rotating Pt–Pt electrode.

Table 2. Comparison of ammonia oxidation catalysts (C_{NH_3} = 100 mg l^{-1} pH 8·00 ± 0·15, SR = 0·2 V min^{-1}, N = 10 rev s^{-1})

Catalyst	*Peak current density* (mA $cm^{-2}{}_{geom}$)
Platinized Pt	2·30
Platinized Graphite*	1·65
Platinum-black coated Ti [70 (mg Pt) cm^{-2}]	0·85
Platinized Ti	0·30
Platinized Ta	0·18

* tested at 50 mg l^{-1} NH_3

current densities obtained with platinum catalysts as a function of substrate material and method of platinum black application.

Treatment procedures of titanium and tantalum prior to platinum electroplating are very critical in view of obtaining an active catalyst coating. We experienced a poor reproducibility and poor stability in work with these catalysts and found powder platinum black catalyst coated on titanium much more attractive in terms of the catalytic activity and stability.

Since cost limitations necessitate a very small quantity of active material, distribution and utilization of the electrocatalyst would be enormously aided by the existence of a diluent which would not adversely affect the properties of the material being diluted.

Graphite, generally used for this purpose, and tungsten bronzes, to which were attributed the property of promoter–diluent for platinum catalysts in some electro-organic reactions, were used as diluents.

A series of electrodes were prepared and tested anodically in an attempt to optimize the catalytic and adhesive properties of the coated layer and to minimize the amount of platinum per unit area of electrode surface.

The effect of Teflon content on the performance of Teflon-bonded platinum electrodes was investigated and the results shown in Fig. 9.

Maximal oxidation rates, obtained with electrodes containing equal amounts of platinum per surface unit but different Teflon content, were observed between 25–30% Teflon content. Oxidation rates decreased with increased Teflon content. This is explained by the prevailing hydrophobic properties of Teflon, which causes poor contact with electrolyte. With increased Teflon content the adhesion of the catalyst layer was increased as expected, but this made a poorer electrode on account of the lower oxidation rates. The region of Teflon content below 20% was not investigated because of poor adhesion to the electrodes. However, Giner *et al.* [11] succeeded

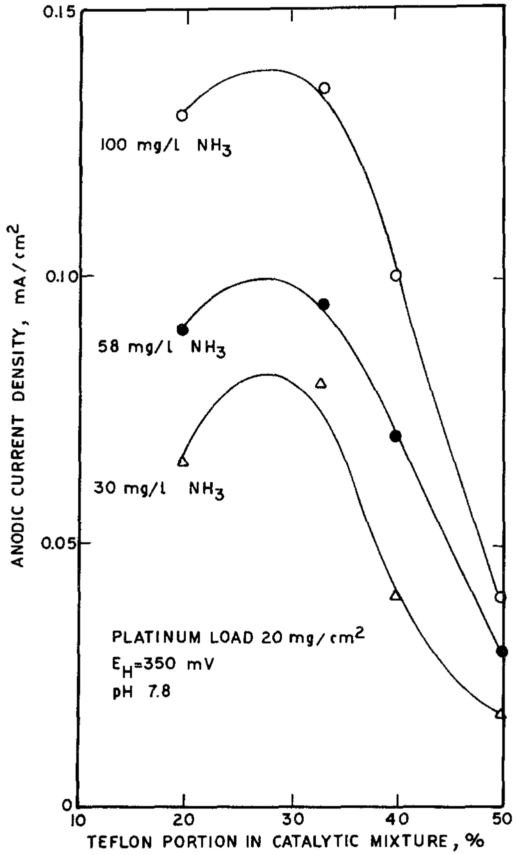

Fig. 9. Effect of Teflon content on performance of Teflon-bonded platinum electrode. Rotating Pt–Pt electrode.

in the preparation of electrodes with Teflon content in the region 10–20% Teflon. They obtained relatively symmetrical curves of current versus Teflon content with low currents at low Teflon content.

The specific activity of the catalyst for the electro-oxidation of ammonia was investigated as a function of platinum loading using tungsten bronze and graphite-containing electrodes with a platinum load of 0·5–20 (mg Pt) cm^{-2}. Electrode performance with tungsten bronzes was erratic and non-reproducible. As a result, the correlation between platinum loading and specific activity was poor. It was not possible to determine whether there was any advantage in lower catalyst loadings. The results with graphite were quite reproducible. The improvement in specific activity with decreased platinum loading was very clear; a six-fold increase in specific activity was observed between 0·5 (mg Pt) cm^{-2} and 20 (mg Pt) cm^{-2}.

The specific activity of graphite-containing platinum black electrodes tested in our experiments at pH = 7·8 ± 0·1, an ammonia concentration of 121 mg l^{-1} and sweep rate of 0·2 V min^{-1} is shown in Table 3. The highest specific activity [over 100 μA (mg Pt)$^{-1}$] is observed at low platinum loadings [0·5 and 1·0 (mg Pt) cm^{-2}]. A substantial decrease in platinum utilization can be observed at increasing platinum loadings. In the range of 4–9 (mg Pt) cm^{-2}, specific activity is about 30 μA (mg Pt)$^{-1}$, and at still higher loadings, [10–20 (mg Pt) cm^{-2}] it drops to about 1/6 of the highest measured values.

Table 3. Specific activity of the electrocatalyst as a function of platinum loading. (SR = 0·2 V min^{-1}, pH = 7·8 ± 0·1, C = 121 mg l^{-1} NH$_3$)

Platinum loading (mg cm^{-2})	*Peak current density* (μA cm^{-2})	*Specific activity* [μA (mg Pt)$^{-1}$]
0·5	56	112
1·0	139	139
2·0	114	57
3·0	120	40
4·0	124	31
5·0	150	30
6·0	174	29
7·0	175	25
8·0	240	30
9·0	270	30
10·0	200	20
15·0	328	22
20·0	360	18

3.2. *Platinized platinum macro-electrode*

The degree of completion of the oxidation reaction, current efficiency, and reaction products, were determined using a larger electrolytic cell with a rotating platinized platinum anode of 20 cm^2 geometric surface area. Tests for nitrites, nitrates, hydrazine, and hydroxylamine using colorimetric methods were negative. Quantitative analysis of evolved nitrogen as the only gaseous product of the electro-oxidation of ammonia was successfully performed using gas chromatography. Known amounts of the head gas from a sealed cell were used to obtain reference peaks on the chromatograms, and were compared with known dilutions of air in helium. Results of the analysis from one experiment are shown in Table 4.

The 'observed I' value of nitrogen evolved refers to the value obtained by gas chromatographic analysis and the 'observed II' value is obtained from the solution ammonia loss during the reaction, assuming stoichiometric conversion of ammonia to nitrogen. Both analytical procedures give reasonably consistent conclusions about the degree of completion of the oxidation reaction and current efficiency, except at the very beginning of the reaction where amounts of the evolved nitrogen are very small, and chromatographic analysis could fail to give accurate results. Current efficiency for the oxidation reaction (with the assumption of three-electron exchange) varied between 50–100% depending upon the experimental conditions and the degree of completion of the oxidation reaction.

3.3. *Continuous flow apparatus*

3.3.1. Cell design. The design equation was derived from a material balance around a differential length of flow path. In this derivation, f_d is the flow rate in ml s^{-1}, C is local concentration in mol l^{-1}, i is current density in mA cm^{-2} and η is current efficiency. L is total flow path length, dL is differential flow path length both in cm, w is path width in cm, F is 96 500 A s mol^{-1} and n is 3.

Table 4. Determination of gaseous reaction products ($C_i = 50$ mg l^{-1} NH_3, pH 8·2, CD = 0·85 mA cm^{-2})

Reaction	*Charge*	*Volume of* N_2 *evolved* (ml)			*Degree of*	*Current efficiency*
time (h)	(C)	*Theoretical*	*Observed I*	*Observed II*	*completion*	η_{av}
2·0	123	4·8	3·5	4·9	0·10	0·88
3·5	214	8·3	7·6	7·1	0·18	0·89
4·5	275	10·6	10·3	–	0·24	0·97
5·0	306	11·8	12·5		0·28	1·06
20	1224	47·3	30·2	24·0	0·78	0·57
25	1530	59·2	33·7	28·5	0·95	0·53

$$f_d C = f_d\,(C + dC) + \frac{\eta i w\,dL}{nF} \tag{2}$$

$$-f_d\,dC = \frac{\eta i w\,dL}{nF} \text{ or } -\frac{dC}{i} = \frac{\eta w\,dL}{f_d nF}. \tag{3}$$

If, as a first approximation, an average current density, which is assumed to be constant along the flow path, is used, Equation 3 can be directly integrated to give:

$$f_d\,(C_i - C_o) = \frac{\eta i_{avg} w L}{nF} \tag{4}$$

where C_i is the concentration at the inlet and C_o is the concentration at the outlet. This approximation was instrumental in setting up the first experimental cell.

To provide a more accurate design equation, the current density, i, must be considered a function of local ammonia concentration, C. Data from the microelectrode study which are quoted in Table 5 were used for this calculation. These data were fitted to six types of relations, each containing two empirical constants. The three which gave the highest degree of correlation were:

$$i = \frac{C}{a + bC}. \tag{5}$$

$$i = a + \frac{b}{C} \tag{6}$$

$$i = aC^b \tag{7}$$

where a and b are the empirical constants. They are not the same in each equation. Final selection was made after evaluating the integral on the left hand side of:

$$-\int_{C_i}^{C_o} \frac{dC}{i} = \frac{\eta w}{f_d nF} \int_0^L dL \tag{8}$$

for several concentration regions.

Table 5. Current density as a function of ammonia concentration at $E_H = 430$ mV, Pt–Pt, pH ~ 8

C (mol l^{-1})	i (mA cm^{-2})
0·01	2·28
0·003	1·83
0·002	1·75
0·001	1·5
0·0006	1·16
0·00012	0·225

Except for Equation 6 which predicts that the cell will be more efficient (i.e., have a shorter flow path) at low concentrations (Table 6), the differences in prediction are relatively small. In the absence of large differences in prediction, Equation 7 was selected, because it gave a design equation from which the empirical constants could be extracted. Assuming that the variation with potential is given by:

$$i = a'\,e^{\phi}\,C^b \tag{9}$$

where ϕ is the electrode potential in V versus SHE, which leads to the design equation:

$$\frac{\eta w L}{f_d nF} = \frac{C_i^{\,1-b} - C_o^{\,1-b}}{a'\,e^{\phi}\,(1-b)}. \tag{10}$$

Analysis of the data, which are given in Table 7, produced a value of 5·6 for a' and b has the experimentally determined value of 0·5.

3.3.2. Cell operation. The results from four typical experiments employing platinum electroplated titanium catalysts and one experiment with commercial powder platinum black catalyst are presented in Table 7. Feed concentrations, volumetric feed rates, and spacer thicknesses were varied from experiment to experiment. Feed con-

Table 6. Values of the integral $\int_{C_i}^{C_o} \mathrm{d}C/i$

C_i (mol l^{-1})	C_o (mol l^{-1})	*Value of integral* $\int_{C_i}^{C_o} \mathrm{d}C/i$ *according to*		
		Equation 5	*Equation 6*	*Equation 7*
0·01	0·001	0·0036	0·0049	0·0041
0·001	0·0001	0·0014	0·00058	0·0013
0·01	0·0001	0·0050	0·0055	0·0054

centrations varied in a narrow range, 27–30 mg l^{-1} ammonia, volumetric feed rates were 70,75,100 and 110 ml h^{-1} and two different spacers were used, 0·1 and 0·05 cm thick. Ammonia conversion increased with increased current density up to a limited value of about 0·4 mA cm^{-2}. Further increase in current density shifted the potential beyond the optimal oxidation potential region and the ammonia consumption started decreasing. An optimal anodic potential is found to be in agreement with previous determinations (microtests), i.e., between 350 and 550 mV versus SHE. With the exception of higher current efficiency at very low current density (η = 0·402 at 0·158 mA cm^{-2}, Table 7A) current efficiency varied between 13·5–28·2% in all experiments with platinum electroplated titanium averaging 22%. This very low current efficiency (calculated from ammonia concentration changes and assuming a three-electron exchange reaction) observed in all of our experiments with a flow through the cell could be attributed to the open cell configuration with closely spaced electrodes, which was used in these experiments. In this configuration cathodic

Table. 7. Experimental data from the continuous-flow electrolytic cell

Current density (mA cm^{-2})	*Potential* E_H (V)	*Effluent concentration* $C_o \times 10^3$ (mol l^{-1})	NH_3 *removal* $(C_i - C_o)/C_i$	*Current efficiency* η
A. Platinum electroplated titanium anode				
(1) $C_i = 1{\cdot}69 \times 10^{-3}$ mol l^{-1}, $f_d = 100$ ml h^{-1}, l.v. = 0·40 cm s^{-1}, $t_R = 227$ s				
0·158	0·352–0·392	1·19	0·296	0·402
0·317	0·432–0·457	1·01	0·402	0·273
0·397	0·502–0·527	0·806	0·523	0·282
0·476	0·702	0·923	0·454	0·205
(2) $C_i = 1{\cdot}6 \times 10^{-3}$ mol l^{-1}, $f_d = 75$ ml h^{-1}, l.v. = 0·30 cm s^{-1}, $t_R = 302$ s				
0·238	0·422–0·437	1·01	0·369	0·238
0·397	0·442–0·457	0·69	0·569	0·220
(3) $C_i = 1{\cdot}78 \times 10^{-3}$ mol l^{-1}, $f_d = 75$ ml h^{-1}, l.v. = 0·30 cm s^{-1}, $t_R = 302$ s				
0·238	0·457–0·502	1·33	0·253	0·181
0·317	0·477–0·522	1·22	0·315	0·169
0·476	0·627–0·682	0·935	0·475	0·170
(4) $C_i = 1{\cdot}78 \times 10^{-3}$ mol l^{-1}, $f_d = 70$ ml h^{-1}, l.v. = 0·55 cm s^{-1}, $t_R = 162$ s				
0·238	0·337–0·362	1·25	0·298	0·198
0·317	0·347–0·352	1·15	0·354	0·177
0·476	0·447–0·557	1·06	0·404	0·135
B. Commercial platinum black catalyst				
30 (mg Pt) cm^{-2} $C_i = 1{\cdot}69 \times 10^{-3}$ mol l^{-1}, $f_d = 110$ ml h^{-1}, l.v. = 0·44 cm s^{-1}, $t_R = 206$ s				
0·238	–	1·29	0·237	0·24
0·397	–	1·00	0·408	0·24

products (mainly evolved hydrogen) could interfer with the anodic reaction, thus decreasing the current efficiency. The cell optimization was difficult due to the complicated kinetics of the reaction. Increased linear velocity had a little effect on the cell performance, which is in agreement with our previous findings about prevailing activation control of the reaction.

Commercial powder platinum catalyst was tested in the continuous flow cell at a platinum loading of about 30 (mg Pt) cm^{-2}. The experiment was carried out at two different current densities, 0·238 and 0·397 mA cm^{-2}, yielding 23–40% ammonia conversion, and proceeding with 24% current efficiency (Table 7B).

No significant change in catalyst activity was observed during the experiment (20 hours).

4. Conclusions

Technically, electro-oxidation has a number of desirable attributes as a means of removal of ammonia during secondary sewage treatment. Under conditions of ammonia concentration and pH typical of treatment effluents, the reaction on platinized platinum catalyst proceeds stoichiometrically to nitrogen with no other oxidation products. Oxidation rates are measureable at concentrations as low as 2 mg l^{-1}. For an electrochemical reaction the cost of power would be very low, about 1 cent per thousand gallons.

However, the only electrocatalyst on which the reaction would proceed with any reasonable rate was platinum. This led to the conclusion that at the present time the capital investment would be too high for the process to be economically feasible.

Because of the technical promise a considerable search was made into possible electrocatalysts. This included a wide variety of metals including noble metals, metal oxides, commercial electrocatalysts and proprietary catalysts. No material was found which was an improvement over platinum. Even with platinum the current density was low which resulted in a large electrode area requirement.(7·2 $ft^2/gal\ h^{-1}$). Specific utilization increased as platinum loading decreased. Some economic advantage resulted from use of extenders like graphite and tungsten bronzes. However, neither of these was sufficient to lower the catalyst cost per unit area to a suitable value.

The total estimated power and capital cost for removal of 20 mg l^{-1} of ammonia with a unit cost of $7·00 per square foot of electrode amounts to 46¢ per thousand gallons of water.

While the process is not economically feasible at the present time, future work may result in the development of a cheaper catalyst, or a catalyst of similar price which would operate at a higher current density or, possibly, a means of even distribution of a very thin layer of platinum black over an electrode surface. Any of these could result in a sufficient economic improvement to enable the process to achieve its considerable promise.

Acknowledgements

The data in this paper were taken from a study supported by the Environmental Protection Agency, Water Quality Office, Project No. 17010 EED. The encouragement and suggestions of Dr C. A. Brunner from this office are gratefully acknowledged. The authors also wish to thank Dr J. Giner for his valuable comments and encouragement in the preparation of this manuscript for publication.

References

[1] T. Katan and R. J. Galiotto, *J. Electrochem. Soc.* **110** (1963) 1022.
[2] H. G. Oswin, and M. Solomon, *Canad. J. Chem.* **41** (1963) 1968.
[3] A. R. Despić, D. M. Dražić and P. M. Rakin, *Electrochim. Acta* **11** (1966) 997.
[4] D. Sparbier and G. Wolf, *Z. Naturforsch* **19a** (1964) 614.
[5] K. Sasaki and Y. Hisatomi, *J. Electrochem. Soc.* **117(6)** (1970) 758.
[6] E. Muller and F. Spitzer, *Z. Elektrochem* **11** (1905) 917.
[7] V. O. Reitlinger, *ibid* **20** (1914) 268.
[8] D. J. G. Ives and G. J. Janz, 'Reference Electrodes' Academic Press, New York (1961).
[9] L. W. Niedrach and I. B. Weinstock, *Electrochem. Technol.* **3** (1965) 270.
[10] M. E. Straumanis, *J. Amer. Chem. Soc.* **71** (1949) 679.
[11] J. Giner, J. M. Parry, S. Smith and M. Turchan, *J. Electrochem. Soc.* **116** (1969) 1692.